

# HOM DAMPED NORMAL CONDUCTING 1.5 GHz CAVITY DESIGN EVOLUTION FOR THE 3RD HARMONIC SYSTEM OF ALBA STORAGE RING

B. Bravo, J. M. Alvarez, A. Salom, F. Perez, CELLS – ALBA, Cerdanyola del Vallès, Spain

## Abstract

In a collaboration framework with CERN, ALBA has designed a normal conducting active 1.5 GHz cavity which could serve as main RF system for the Damping Ring of CLIC and as an active third harmonic cavity for the ALBA Storage Ring (SR). The third harmonic cavity at ALBA will be used to increase the bunch length in order to improve the beam lifetime and increase the beam stability thresholds. The main advantage of an active third harmonic cavity is that optimum conditions can be reached for any beam current. This paper presents the evolution of the preliminary design of this cavity and its trans-dampers: high order modes coaxial dampers with waveguide transitions to N, which allows extracting the power of the high order modes induced by the beam outside of the cavity and to dissipate it using standard loads. This approach has two main advantages: no ferrites brazing is needed and they provide a diagnostic to analyse the beam dynamics. The new features of the design, together with electromagnetic simulations, mechanical and thermal stress analysis will be presented in this paper as well as the first stages of the prototype production status.

## INTRODUCTION

The fundamental RF system of ALBA SR is based on normal conducting high order mode damped cavities working at 499.654MHz [1,2] and fed by IOT power amplifiers.

For the RF 3<sup>rd</sup> Harmonic System of ALBA SR a similar system, based on normal conducting high order mode damped cavities, will be employed [3].

The main advantage of an active third harmonic system in opposition to passive super conducting cavities is that optimal beam lengthening conditions can be achieved regardless the beam current [4,5].

Table 1 summarizes the main design parameters of the 3<sup>rd</sup> Harmonic Cavity (3HC) of ALBA to achieve the optimum conditions at maximum SR current.

## CAVITY DESIGN

CST 3D Simulation Software has been used to optimize the design of the cavity.

### Beam Pipe Radius

The beam pipe radius was the first constraints considered for this design and it was defined by the beam aperture of the present lattice of ALBA SR, determined by the scrapper position to protect the In-Vacuum Undulators. The 3<sup>rd</sup> Harmonic section will be placed in a straight section with small dispersion and  $\beta_{y,cav} = 5.15m$  and  $\beta_{x,cav} = 9.18m$ . The minimum beam pipe radius is determined by the half-aperture requirement at the cavities as shown in Eq (1):

$$\frac{r_{scrapper}}{\sqrt{\beta_{y,scrapper}}} < \frac{r_{pipe}}{\sqrt{\beta_{y,cav}}} \Rightarrow r_{pipe} > \frac{r_{y,scrapper} \sqrt{\beta_{y,cav}}}{\sqrt{\beta_{y,scrapper}}} = 4.4mm \quad (1)$$

A safe margin of 2.5 times respect to the minimum pipe radius was considered and the closest standard conflat flange was selected, which in this case was CF35 with 23mm of diameter.

Table 1: Third Harmonic Cavities Requirements

Parameter	Value
Total Voltage	1.1MV
Frequency	1.49896GHz
BBU threshold	> 400mA
HOM Longitudinal Z	< 5 MOhms. MHz
HOM Transversal Z	< 50kOhms/m
Nominal/Max power	16/20 kW
Number of cavities	4

### Cavity Geometry Optimization

Figure 1 represents the transverse cut of a quarter of the 3HC. It shows the main geometrical parameters considered for its optimization, where Quality Factor (Q), Shunt Impedance ( $R_s$ ) and Resonance Frequency ( $f_r$ ) are the parameters to optimize.

The gap width (g) results from a trade-off between transient-time factor and electric field, integrated along the axis. The shunt impedance shows strong dependence of the nose-cone radius ( $r_{nose}$ ) and a weak dependence on the nose-cone angle (angle<sub>nose</sub>).

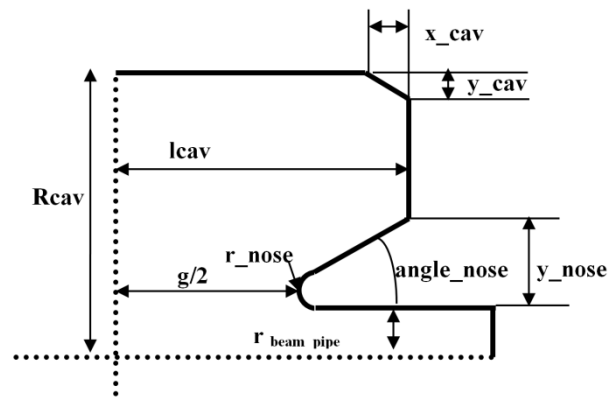


Figure 1: One quarter of ALBA 3<sup>rd</sup> Harmonic Cavity and main geometrical constraints.

The radius of the nose is the parameter with highest impact on the shunt impedance, and thus, on the achievable voltage of the cavity. However, this voltage is limited by the RF breakdown is defined by Kilpatrick criterion shown in Eq (2):

Content from this work may be used under the terms of the CC BY 3.0 licence (© 2019). Any distribution of this work must maintain attribution to the author(s), title of the work, publisher, and DOI

$$|E|e^{-4.25/E} = 24.4 \cdot \sqrt{f(\text{GHz})} \quad (\text{MV/m}) \quad (2)$$

For the 3HC of ALBA, the maximum electric field before achieving this RF breakdown would be 34MV/m.

After optimizing all the geometrical parameters of the cavity, simulations shows that with an optimum nose radius of 3mm, the maximum field would be 16MV/m.

### Optimization of the dampers

Once the optimization of the body of the cavity was finished, the dampers were studied and optimized. In order to avoid the use of ferrites and brazing to absorb the power of the HOM, a waveguide to N transition was included in the dampers, the device has been named “TransDamper”. In this way, the power of HOM can be extracted from the dampers and also analyzed. In overall, there are three dampers in the cavity and each of them is composed of three parts:

- A circular waveguide with ridges.
- A transition from circular to rectangular waveguide.
- A transition from rectangular waveguide to N.

#### Circular Waveguide

The  $f_c$  of a circular waveguide of diameter  $r_{\text{damper}}$  is given by Eq (3):

$$f_c = \frac{1.812c}{2\pi r_{\text{damper}}} = 2.6\text{GHz} \quad (3)$$

By including rectangular ridges in the waveguide, the cut-off frequency can be further reduced. Figure 2 shows the dimensions of the ridges to be optimized.

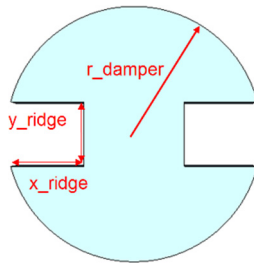


Figure 2: Transverse profile of damper circular waveguide and ridges.

Figure 3 shows how the cut-off frequency decreases when ridges dimensions increase. These dimensions were optimized to have 1.72GHz cut-off frequency.

#### Rectangular Waveguide

The cut-off frequency of the rectangular waveguide has to be as closed as possible to the  $f_c$  of the circular ridge waveguide. Following Eq (4)

$$f_{c, \text{rectangular}} = \frac{c}{2\pi} \sqrt{\left(\frac{m\pi}{a}\right)^2 + \left(\frac{n\pi}{b}\right)^2} = \frac{c}{2a} \quad (4)$$

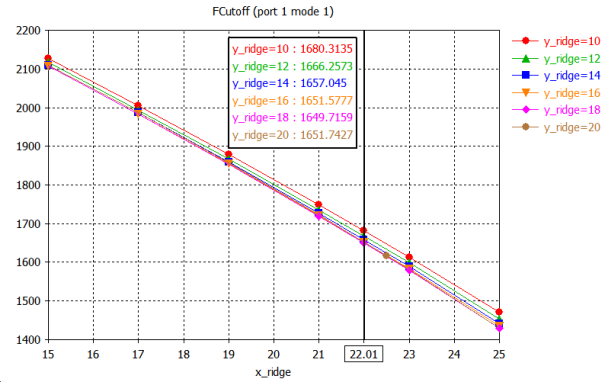


Figure 3: Variation of cut-off frequency of dampers versus ridges dimensions.

#### Circular to Rectangular Waveguide Transition

A variety of methods exist for transforming circular waveguide propagating TE<sub>11</sub> mode to a rectangular waveguide propagating TE<sub>10</sub> mode. The adopted solution is a gradual transition in which the circular cross section is transformed continuously over the length of the transition into a rectangular cross section

Figure 4 shows the field lines of TE<sub>11</sub> and TE<sub>10</sub> modes of circular and rectangular waveguides respectively and Fig 5. shows the transition that gradually transforms the TE<sub>11</sub> to TE<sub>10</sub>.

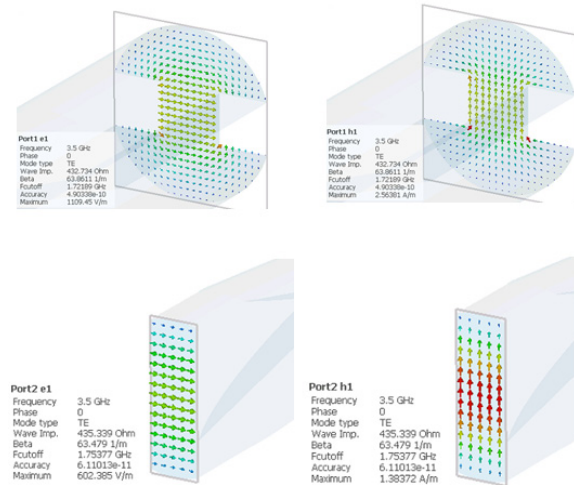


Figure 4: Field Lines of TE<sub>11</sub> mode of circular waveguide (top) and field lines of TE<sub>10</sub> mode of rectangular waveguide (bottom) after gradual transition.

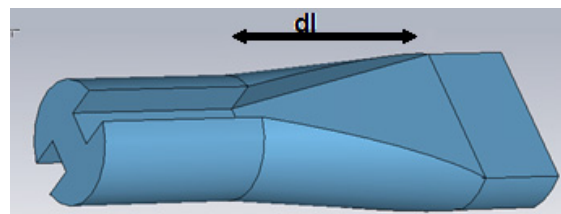


Figure 5: Transition from ridged circular waveguide to rectangular.

Content from this work may be used under the terms of the CC BY 3.0 licence (© 2019). Any distribution of this work must maintain attribution to the author(s), title of the work, publisher, and DOI

An important parameter for getting a low insertion loss is the length of the transition (d1). This parameter was optimized for minimum insertion loss and minimum length. The longer the transition is, the lower the insertion loss. A compromise between minimum length and a low insertion loss is gotten for d1=130mm

### Waveguide to N transition

A feed-through port with N connector has been added at the end of the rectangular waveguide. An external load will be connected here to dissipate the power generated by the HOM of the cavity. A second port for a cold-cathode gauge has been added. The dimensions of these ports and the antenna of the N-connector have been optimized to maximize  $S_{21}$  between 1.7GHz and 5GHz.

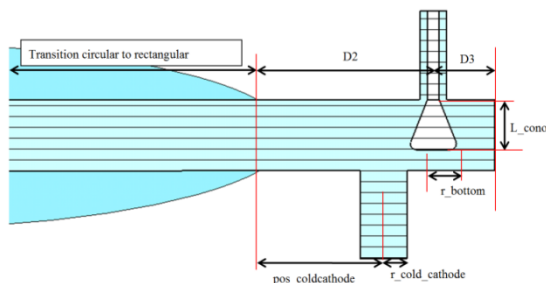


Figure 6: Optimization of Waveguide to N transition of trans-dampers.

After optimization of parameters shown in Fig. 6, the estimated  $S_{21}$  of the N port is below -0.2dB between 2GHz and 5GHz. To further improve this value, a stub has been added opposite to the cold cathode port, achieving values lower than -0.1dB for  $S_{21}$  as shown in Fig. 7.

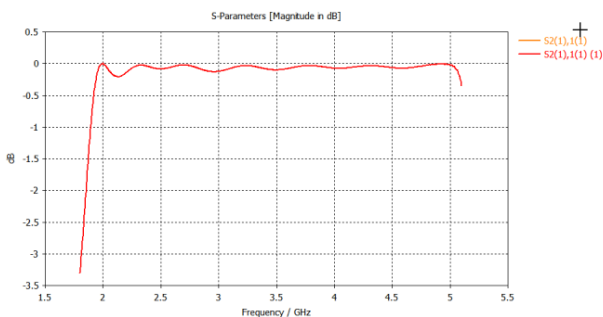


Figure 7:  $S_{21}$  of trans-damper between 2GHz and 5GHz.

## CAVITY MECHANICAL DESIGN

### Fluid Thermal Simulations

Coupled thermal-fluid simulations have been performed, using Siemens NX as FEA package. The surface heat deposition, calculated with the electromagnetic model, has been imported as a heat load distribution. Flowing through the cavity body, the cavity body lids and dampers, water at 23 °C is used as coolant.

Figure 8 shows the result of temperature distribution in the cavity. In the picture is shown the cavity sectioned

making visible the nose cone and the damper ridges. Is precisely in the damper ridge edge where the temperature reaches its maximum value, 66.7 °C.

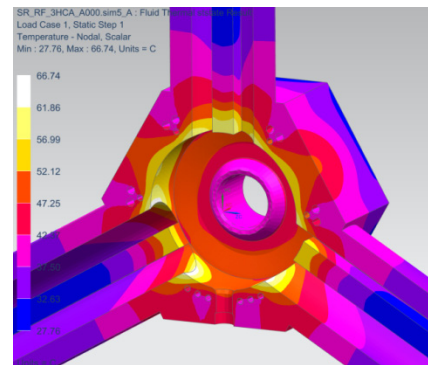


Figure 8: Cavity temperature distribution.

Other critical components of the cavity were analysed like the input coupler, cooled by air and water and the tuner for adjustment of resonance frequency.

Figure 9 shows the maximum temperature reached in the external part of the input coupler (55°C) cooled by water and in the surroundings of the ceramic cooled by air (33°C).

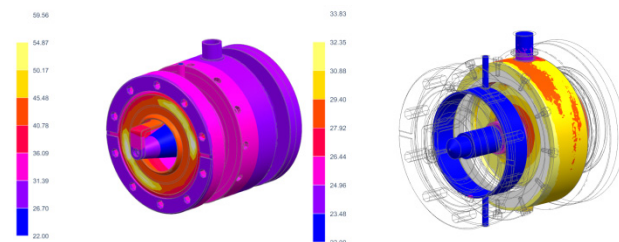


Figure 9: Temperature distribution of input coupler, cooled by water (left) and of ceramic surroundings, cooled by air (right).

## PRODUCTION STATUS

The tender for the construction of the 1<sup>st</sup> cavity prototype was released in December 2018.

Low and high power tests are expected to be done by the end of 2020.

## CONCLUSIONS

Electromagnetic and Mechanical simulations of the 1.5GHz third harmonic active cavity have proven the feasibility of this project.

The design of the wide broadband trans-dampers with N transitions connected to external loads will avoid the use of ferrites and brazing, making easier the construction phase and reducing the risks associated to ferrites failures. Moreover, it will provide a diagnostic tool of the HOM of the beam.

## ACKNOWLEDGMENTS

This work was supported by a collaboration agreement between the CERN CLIC project and ALBA, contract number KE2715/BE/CLIC.

## REFERENCE

- [1] E.Weihreter, V.Dürr, F. Marhauser, “A ridged circular waveguide ferrite load for cavity HOM damping”, presented at *EPAC 2006* Edinburgh, Scotland paper TUPCH14.
- [2] M. Langlois, M. Cornelis, F. Perez and D. Einfeld, “RF measurements on variations of the ALBA Dampy cavity”, *Proceedings of PAC09*, Vancouver, BC, Canada.
- [3] B.Bravo, J.Alvarez, A.Salmon, F. Ferez, “1.5 GHz cavity design for the CLIC Damping Ring and as active third harmonic cavity for ALBA”, *Proceedings of IPAC2017*, Copenhagen, Denmark.
- [4] A. Hofmann and S. Myers, “Beam dynamics in a double RF system”, *Proc. of the 11th Int. Conf. on High Energy Acc.*, ISR-TH-RF/80-26, 1980.
- [5] ,R. Biscardi\*, S.L. Kramer, G. Ramirez, “Bunch length control in the NSLS VUV ring” *Nuclear Instruments and Methods in Physics Research A* 166 (1995) 26-30.